PERSPECTIVE

Dalton
www.rsc.org/dalton

Diffusion and NOE NMR spectroscopy. Applications to problems related to coordination chemistry and homogeneous catalysis †

Paul S. Pregosin, Eloísa Martínez-Viviente and P. G. Anil Kumar
Laboratory of Inorganic Chemistry ETHZ, Hönggerberg, CH-8093 Zürich, Switzerland

Received 6th May 2003, Accepted 10th June 2003
First published as an Advance Article on the web 22nd September 2003

A novel NMR approach involving PGSE diffusion measurements to elucidate problems related to molecular volume, hydrogen bonding and ion pairing is suggested. When combined with heteronuclear NOE data, one obtains a much more detailed understanding of how anions and cations interact in complex salts.

Introduction

NMR spectroscopy represents a major structural tool for the inorganic/organometallic chemist. Apart from the usual one-dimensional conventional NMR spectrum, the community has slowly adjusted to cross-peaks (from 2D NOESY and related studies). In addition to our NMR program on NOE spectroscopy, we have become interested in diffusion studies, as these offer a somewhat unique view of molecular size and inter- and intra-molecular interactions.

The determination of relative molecular size represents a subject of considerable interest to the coordination chemistry community with respect to the formation of polynuclear complexes, ion pairs and otherwise aggregated species. Apart from classical methods such as mass spectrometry and those based on colligative properties, the Pulsed Field Gradient Spin-Echo (PGSE) methodology[1,2] has recently resurged as a promising technique. PGSE measurements, introduced more than 30 years ago by Stejskal and Tanner,[3] make use of the translational properties of molecules, which are directly responsive to molecular size and shape. Applications in coordination and/or organometallic chemistry remain sparse,[4–14] but are on the increase.

A PGSE NMR diffusion measurement consists of a spin-echo sequence in combination with the application of pulsed field gradients. The two most common sequences are shown in Fig. 1.

In the Stejskal–Tanner experiment,[1] Fig. 1a, transverse magnetization is generated by the initial π/2 pulse which, in the absence of field gradients, dephases due to chemical shift, hetero- and homonuclear coupling evolution, and spin–spin (T_2) relaxation. After application of an intermediate π pulse, the magnetization refocuses, generating an echo. The first pulsed linear field gradient results in strong dephasing of the magnetization with a phase angle proportional to the length (δ) and the amplitude (G) of the gradient. Because the strength of the gradient varies linearly along, *e.g.*, the z-axis, only spins contained within a narrow slice of the sample acquire the same phase angle. The second gradient pulse, which must be exactly equal to the first, reverses the respective phases and the echo

† Based on the presentation given at Dalton Discussion No. 6, 9–11th September 2003, University of York, UK.

Paul Pregosin was born in New York City in 1943 and received his PhD from the City University of New York in 1970. After postdoctoral studies at Queen Mary College in London, UK and the University of Delaware in Newark, he moved to the ETHZ in 1973 where he has remained ever since. His research interests include organometallic chemistry, homogeneous catalysis and NMR spectroscopy.

Eloísa Martínez-Viviente was born in Cartagena, Spain, in 1974. She graduated from the University of Murcia in 1997 and received the Spanish National Graduation Award in Chemistry for that year. She was involved in student exchange programs which took her first to Oxford with Dr John Brown and then to Zurich, before completing her PhD studies in 2001 with Prof. José Vicente and Dr José A. Abad at the University of Murcia. She is currently doing postdoctoral research in Zurich on the applications of NMR and, especially, PGSE diffusion studies, to problems in Organometallic Chemistry.

P. G. Anil Kumar was born in Chickmagalur, India, in 1977. He received his MSc degree in Inorganic Chemistry from Bangalore University in 1999. After working as a research associate in a project sponsored by AICTE in B.M.S.C.E., he moved to the Indian Institute of Science, Bangalore to work as a NMR Project Assistant in the SIF department. He started his PhD studies in the group of Prof. Pregosin in January 2002. He is currently working on structural and dynamic studies on chiral organometallic complexes and PGSE diffusion studies using NMR as a tool.

Paul S. Pregosin

Eloísa Martínez-Viviente

P. G. Anil Kumar

DOI: 10.1039/b305046g

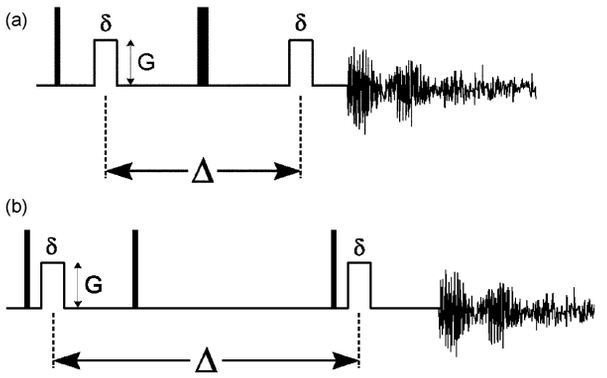

Fig. 1 Typical pulse sequences for the PGSE experiments: (a) the Stejskal–Tanner experiment; (b) the Stejskal–Tanner experiment, modified *via* substitution of two 90° pulses for a single 180° pulse.

forms in the usual way. If, however, spins move out of their slice into neighbouring slices *via* Brownian motion, the phase they acquire in the refocusing gradient will not be the one they experienced in the preparation step. This leads to incomplete refocusing, as in the T_2 dephasing, and thus to an *attenuation* of the echo amplitude. As smaller molecules move faster, they translate during the time interval Δ into slices further apart from their origin, thus giving rise to smaller echo intensities for a given product of length and strength of the gradient.

The stimulated echo experiment, shown in Fig. 1b, is similar[15] except that the phase angles which encode the position of the spins are stored along the *z*-axis in the rotating frame of reference by the action of the second π/2 pulse. The transverse magnetization and the respective signal phases are restored by the third π/2 pulse. This method is advantageous in that during time Δ, T_1, as opposed to T_2, is the effective relaxation path. Since T_1 is often longer than T_2, a better signal/noise ratio is obtained.

The PGSE experiment is usually performed by repeating the sequence while systematically changing either the time allowed for diffusion (Δ), the length (δ) or the strength (G) of the gradient. The diffusion constant, D, can be derived

$$\ln\left(\frac{I}{I_0}\right) = -(\gamma\delta)^2 G^2 \left(\Delta - \frac{\delta}{3}\right) D \qquad (1)$$

G = gradient strength, Δ = delay between the midpoints of the gradients, D = diffusion coefficient, δ = gradient length

from eqn. (1): from the slope of the regression line by plotting $\ln(I/I_0)$ (I/I_0 = observed spin echo intensity/intensity without gradients) *vs.* either $\Delta - \delta/3$, δ^2 ($\Delta - \delta/3$) or G^2, depending on the parameter varied in the course of the experiment.‡ Compounds with smaller hydrodynamic radii move faster, and reveal larger diffusion coefficients. A typical example is given in Fig. 2 for several different anions of a Ru(II) Binap complex.

The D-value can be related to the hydrodynamic radii of the molecules *via* the Stokes–Einstein eqn. (2) and this allows for a viscosity correction.

‡ We estimate the error in D to be ± 0.1 (although the precision is ± 0.06). Heteronuclei such as ^{35}Cl and ^{7}Li usually have short relaxation times and small gyromagnetic ratios, γs. If the same parameters as for ^{1}H and ^{19}F are used, nuclei with small γs result in regression lines whose slopes are too small to be useful. To compensate for this, longer diffusion times (Δ) or longer gradients (δ) can be used. For nuclei with short T_1s (or T_2s), the second alternative (longer gradients) is the most feasible, since small Δ-values are desirable to avoid complete relaxation. The value of δ (which can be *ca.* 10–20 ms) can then be the limiting factor with respect to minimizing Δ.

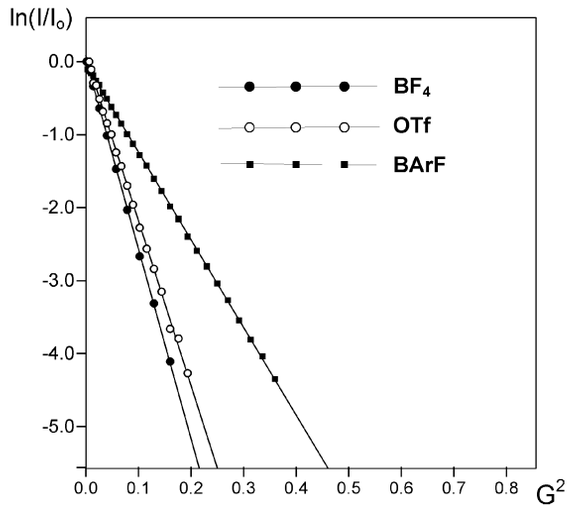

Fig. 2 Plots of $\ln(I/I_0)$ *vs.* arbitrary units proportional to the square of the gradient amplitude for ^{19}F-PGSE diffusion measurements on several salts of the Ru(II) *p*-cymene Binap complexes **15**. The larger the anion the smaller the absolute value of the slope.

$$D = \frac{kT}{6\pi\eta r_H} \qquad (2)$$

k = Boltzmann constant, T = absolute temperature, η = viscosity, r_H = hydrodynamic radius

Molecular volumes

The most obvious application for D-values involves detecting unexpected molecular volumes. There are examples involving ferrocene-based dendrimers, Cu-clusters and Pt(II) molecular squares (and other aggregates), amongst others, and this subject has been reviewed.[14] However, the complexes described in this Perspective were all studied in Zürich. Our initial PGSE measurements involved only ^{1}H NMR studies. Specifically, for **1**, which arises due to incomplete reaction of a methyl Duphos compound with a ruthenium *p*-cymene dinuclear complex,[13] the observed D-value is found to be *ca.* 9–10% larger than that measured for a suitable model complex, thereby supporting the larger molecular volume. Clearly, for **1**, there are separate ^{1}H and ^{13}C *p*-cymene resonances for the two different metal centres and these provide a strong indication of the correct structure.

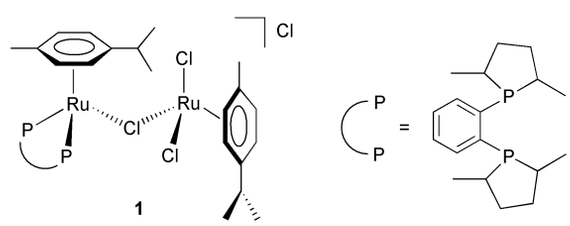

In connection with some of our P–C bond splitting chemistry[16] we have found that both Binap and MeO-Biphep related complexes of ruthenium, **2**, afford interesting dinuclear hydroxy phosphine derivatives, **3**, by addition of water across P–C bonds (see Scheme 1). Originally, for **3**, we considered the mononuclear 16e-species **4** as the correct structure; however, the PGSE measurements shown in Fig. 3 (and later, unpublished X-ray studies), confirm that the di-nuclear formulation is correct. The di-methoxy analog of **4**, complex **5**, is a mononuclear species. The diffusion results reveal that **3a** and **3b** have much larger volumes than **5**, in keeping with the mass spectroscopic data. Moreover, the ratio of the diffusion constants **5/3a**, 0.77, is consistent with *ca.* twice the volume for **3a**.[14] There are

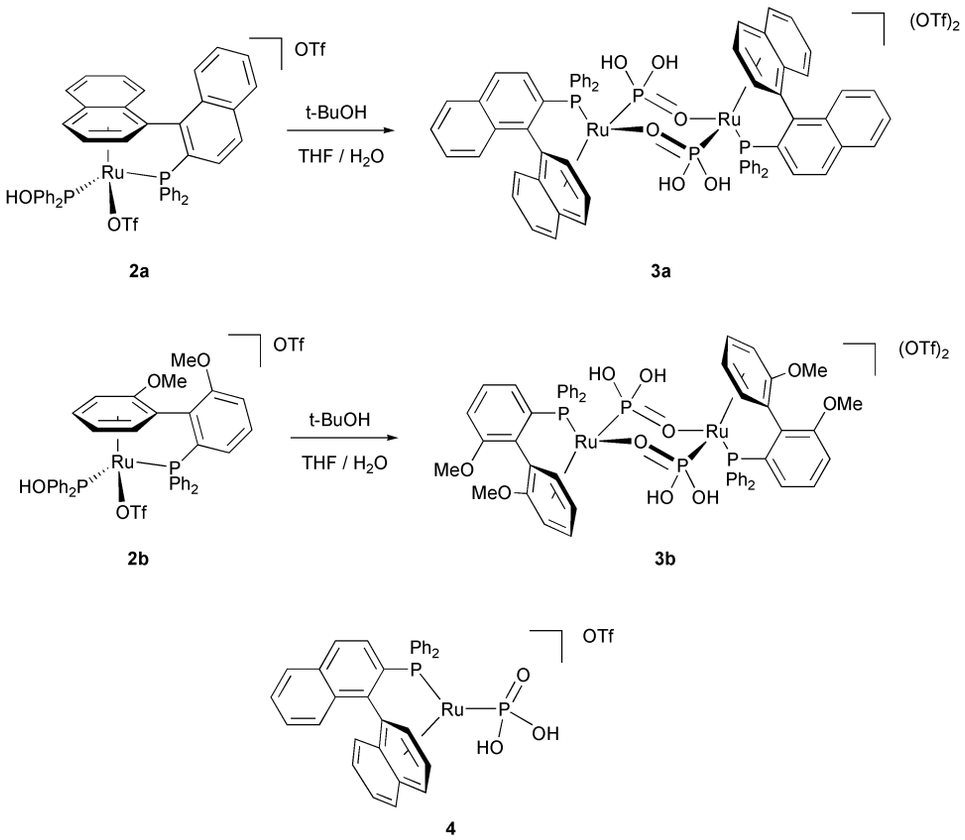

Scheme 1 Hydroxyphosphine complexes of Ru(II).

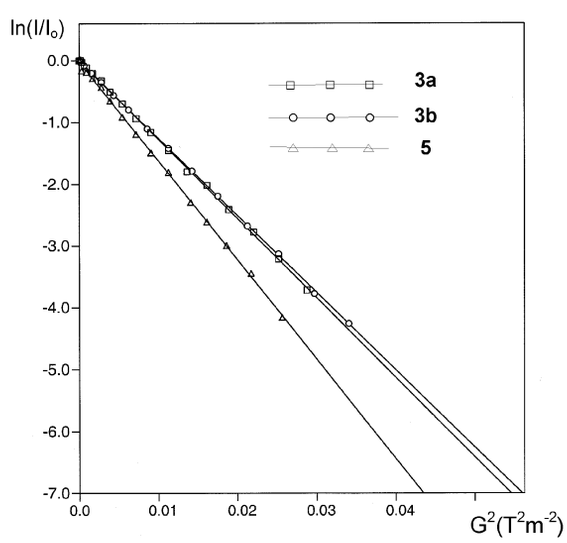

Fig. 3 Plot of the $\ln(I/I_0)$ *vs.* the square of gradient amplitude (expressed in T^2 m^{-2}), for **3a**, **3b** and **5**. The larger slope for **5** is indicative of a smaller molecular volume (see text).

not many examples of $P(=O)(OH)_2$ ligands functioning as P-donors to a transition metal.

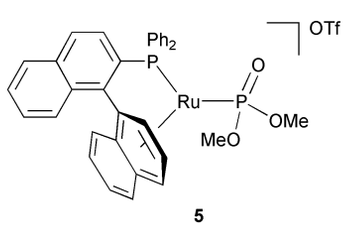

5

Similar studies[13] help to confirm that the binol-based diphosphite ligand, **6**, shown, is not capable of chelating transition metals, since the *p*-thiophenol spacer is too large. However, **6** readily bridges two Ru-metal centers affording dinuclear Ru–arene species such as $[(\eta^6\text{-}C_6H_6)RuCl_2]_2(\mu\text{-}P_2S)$, **7**, and $[(\eta^6\text{-}p\text{-cymene})RuCl_2]_2(\mu\text{-}P_2S)$, **8**.

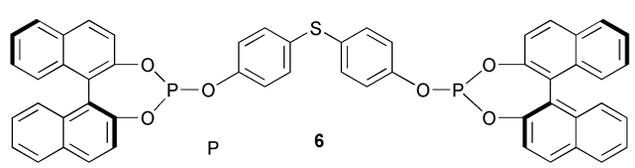

P **6**

Hydrogen bonding

To this point our discussion has concentrated exclusively on the applications of proton PGSE results. However, a relatively large number of cationic ruthenium compounds (and palladium and rhodium. . . *etc.*) are currently in use in homogeneous catalysis and/or organic synthesis. Frequently, these complexes possess anions such as PF_6^-, BF_4^-, $CF_3SO_3^-$ or $BArF^-$. For these, and other complexes, ^{19}F represents an important complement to ^1H PGSE methods. In principle, one can measure the diffusion constants for the cation and anion separately and thus determine whether or not these interact. This allows one to explore possible hydrogen bonding in metal complexes.

Fig. 4 shows ^{19}F PGSE data for both triflate moieties of the cationic compound **2a**, in which there are two different triflate anions.[17] The two lines in the figure are so closely overlapped that these are not visibly readily resolved, suggesting that *both* triflates in **2a** are moving at the same rate. The observed diffusion data from the ^{19}F study are in excellent agreement with those found from the ^1H PGSE study using the protons of the cation. Although one could imagine tight ion-pairing as an explanation for the observed identical diffusion coefficients, we note that the solid-state structure[17] for **2a** suggests an H-bond from the $P(OH)Ph_2$ fragment to the anionic (and not to the complexed) triflate. Consequently, the anionic triflate is most likely carried with the cation *via* the OH-group.

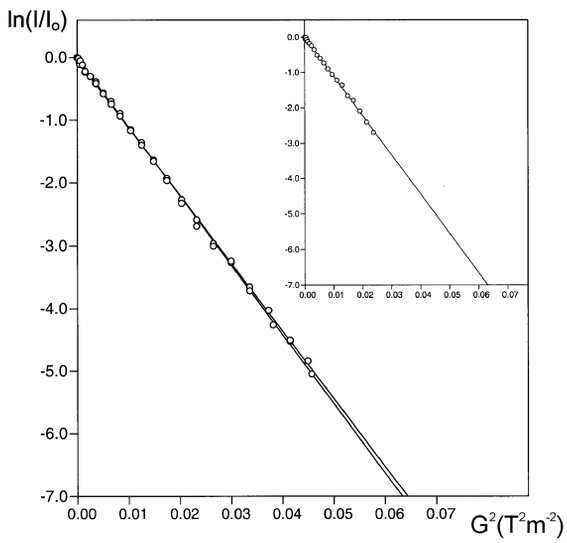

Fig. 4 Plot of the $\ln(I/I_0)$ *vs.* the square of gradient amplitude (expressed in $T^2\ m^{-2}$), for **2a** in $CDCl_3$ using the ^{19}F resonances and, in the smaller box, ^1H signals. The almost equivalent slopes suggest that both triflate anions are moving at the same rate. The slope measured using ^{19}F, corrected for γ_F, is equal (within the experimental error) to that estimated *via* ^1H.

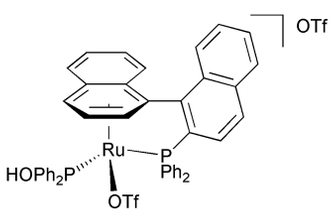

2a

The tungsten adamantol complex $[W(Cp)(1\text{-adamantol})(CO)_3](CF_3SO_3)$, **7**, forms through ionic hydrogenation of the corresponding adamantone by reaction with $[WH(Cp)(CO)_3]$ and triflic acid.[18] The crystal structure of the related $[W(Cp)(CO)_3(HO^iPr)](CF_3SO_3)$ shows hydrogen bonding between the alcohol OH proton and an oxygen of the triflate anion.[18] ^1H NMR data for **7** suggest that this bond is also present in solution and it should be possible to confirm this by ^1H and ^{19}F-PGSE diffusion measurements. However, **7** is not stable at ambient temperature and decomposes within hours to yield free adamantol and $[W(Cp)(CF_3SO_3)(CO)_3]$. Consequently, diffusion data for **7** were obtained at 231K (in CD_2Cl_2), at which temperature the complex is stable. As can be seen from Table 1, the $CF_3SO_3^-$ anion in salt **7** (in CD_2Cl_2) moves at the same rate as the tungsten cation due, presumably, to the presence of hydrogen bonding.

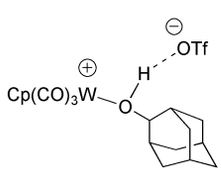

7

Low temperature PGSE diffusion measurements (using the usual flow of cold nitrogen to cool the tube) present technical difficulties, as there is no trivial method to avoid convection.[19] Regrettably, the convection (which moves the molecules) results in incorrect *D*-values unless special precautions are taken.[19]§

§ Convection results in relatively large *D*-values, which increase if larger diffusion times (Δ) are used. Correct *D*-values, on the contrary, are not Δ-dependent.

Table 1 *D*- and r_H-values for **7**[a] in CD_2Cl_2 at 231 K

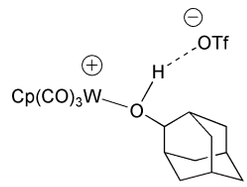

Fragment	Δ/ms	D^b	$r_H{}^c$/Å
Cation (^1H)	118	3.88, 3.87	4.7
	168	3.91, 3.90	4.6
	268	3.93, 3.95	4.6
Anion (^{19}F)	118	3.87, 3.84	4.7
	168	3.84, 3.89	4.7
	268	3.95, 3.94	4.6

[a] 10mM. [b] $\times 10^{10}\ m^2\ s^{-1}$. Estimated using the diffusion coefficient of HDO in D_2O as ref. 33. Standard deviation is *ca.* 6. Results from two different samples and with three different Δ-values, showing the absence of a convection-related Δ-dependence of *D*. [c] Standard deviation is *ca.* 1. $\eta(CH_2Cl_2, 231\ K) = 0.933\ kg\ s^{-1}\ m^{-1}$.

Assuming that one makes the effort to suppress convection, reliable ^1H and ^{19}F diffusion data, *e.g.*, for **7**, can be obtained. To confirm that convection is minimal, measurements with three different Δ-values, for two samples, were made, and that is why Table 1 has rather more data than one might expect.

Occasionally one is happy to know what is *not* responsible for a perhaps unexpected result. The Pd(II)-hydride, **8**, is thought to be the active catalyst in the palladium-catalyzed methoxycarbonylation of ethene to methylpropanoate, where methanol is the solvent of choice.[20] Stable palladium hydride complexes are very rare, and almost never occur with hydride *trans* to phosphorus in square planar complexes. Given the additional dynamic processes that might arise from solvent exchange, the relative stability of **8** is noteworthy. One might think that perhaps the $CF_3SO_3^-$ anion coordinates and/or stabilizes **8** *via* H-bonding to the complexed solvent molecule.

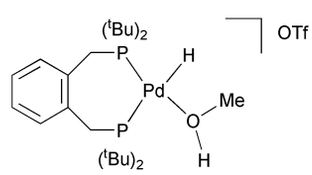

8

To test this idea, diffusion data for **8** in methanol were collected at 240 K (where the compound is stable for prolonged periods) using ^{31}P (instead of ^1H) as a diffusion probe for the cation.[19] The use of this spin, and low temperature diffusion in general, requires some special attention.[19,21] We have found that the best results, in terms of shape and intensity of the detected ^{31}P signals, are obtained using the Stejskal–Tanner sequence (Fig. 1a) and setting the evolution time before and after the 180° pulse to $1/2J_{PP} = 29$ ms.[19] Fig. 5 shows the good quality of the plots obtained from the ^{31}P and ^{19}F (for the anion) low temperature diffusion measurements on **8**. The *D*-values and hydrodynamic radii are shown in Table 2. The results show that the cation and anion are moving at very different rates. Clearly, there is *no* strong hydrogen bond between cation and anion in **8**.

In many cases the *D*-values will reflect an average; nevertheless these results can be informative. Table 3 shows PGSE diffusion data for the Ru–aqua complexes[22] $[Ru(H_2O)_3(CO)(dppe)]X_2$, X = BF_4^- (**9a**), $CF_3SO_3^-$ (**9b**), SbF_6^- (**9c**) and $N(O_2SCF_3)_2^-$ (**9d**), in acetone and water. Comparing the *D* and *r* values for **9a**–**d** in both water and acetone solutions, one finds that the BF_4^-, $CF_3SO_3^-$ and $N(O_2SCF_3)_2^-$ anions are all much

Table 2 *D*- and r_H-values for **8**[a] in CH_3OH[b] at 240 K

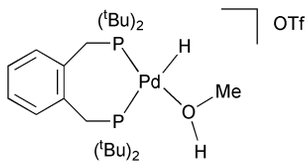

Nucleus	*D*[c]	r_H[d]/Å
Cation (^{31}P)[e]	2.19	5.2
Anion (^{19}F)	3.97	2.9
Anion (^{19}F)[e]	3.97	2.9

[a] 20 mM. [b] Plus three drops of CD_3OD for the lock. [c] × 10^{10} m^2 s^{-1}. Estimated using the diffusion coefficient of HDO in D_2O as ref. 33. Standard deviation is *ca.* 6. [d] Standard deviation is *ca.* 1. η(MeOH, 240 K) = 1.53 kg s^{-1} m^{-1}. [e] Measured with the Stejskal–Tanner sequence (Fig. 1a).

Table 3 *D*- and r_H-values for **9a–d**[a] in $(CD_3)_2CO$ and D_2O

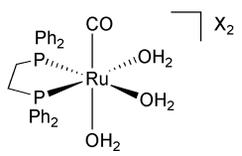

		$(CD_3)_2CO$		D_2O	
Compound	Fragment	*D*[b]	r_H[c]/Å	*D*[b]	r_H[c]/Å
9a BF_4	Cation (^{1}H)	9.36	7.7	3.44	6.2
	Anion (^{19}F)	19.88	3.6	15.29	1.4
9b OTf	Cation (^{1}H)	9.24	7.8	3.47	6.1
	Anion (^{19}F)	15.58	4.6	9.25	2.3
9c SbF_6	Cation (^{1}H)	9.95	7.3	3.30	6.5
9d $N(O_2SCF_3)_2$	Cation (^{1}H)	9.31	7.7	3.43	6.2
	Anion (^{19}F)	17.59	4.1	6.74	3.2

[a] 2 mM. [b] × 10^{10} m^2 s^{-1}. Estimated using the diffusion coefficient of HDO in D_2O as ref. 33. Standard deviation is *ca.* 6. [c] Standard deviation is *ca.* 1. η(300 K, kg s^{-1} m^{-1}): H_2O: 1.03; $(CH_3)_2CO$: 0.303.

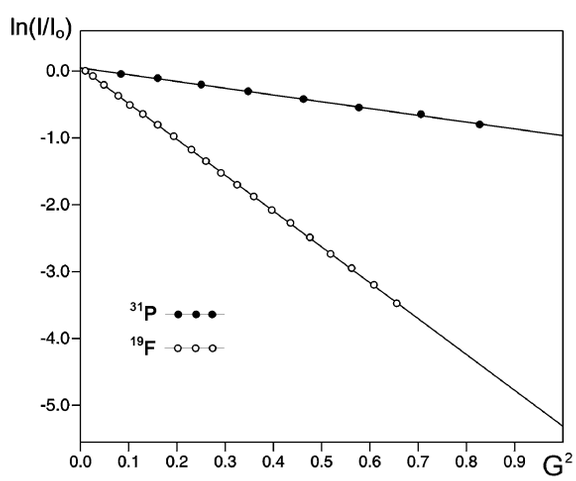

Fig. 5 Plots of $\ln(I/I_0)$ *vs.* arbitrary units proportional to the square of the gradient amplitude for a ^{31}P- (black circles) and a ^{19}F- (white circles) PGSE diffusion measurement on a 20 mM CD_3OD solution of palladium hydride **8**, at 240 K.

smaller in water than in acetone solutions (the ^{19}F resonance of the SbF_6^- is not readily measurable). Indeed, for these three salts, the cations in water reveal reduced radii by *ca.* 1.5–1.6 Å.

Table 4 *D*- and r_H-values for **10** and **11** in CD_2Cl_2 and $CDCl_3$

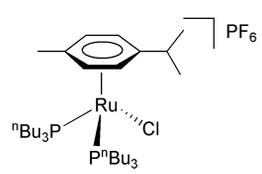

10

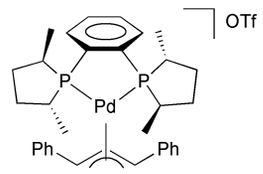

11

		CD_2Cl_2		$CDCl_3$	
Compound	Fragment	*D*[a]	r_H[b]/Å	*D*[a]	r_H[b]/Å
10	Cation (^{1}H)	8.74	6.2	6.25	6.3
	PF_6 (^{19}F)	10.17	5.3	6.27	6.3
11	Cation (^{1}H)	9.14	5.9	6.64	6.0
	OTf (^{19}F)	11.69	4.7	6.45	6.1

[a] × 10^{10} m^2 s^{-1}. Estimated using the diffusion coefficient of HDO in D_2O as ref. 33. Standard deviation is *ca.* 6. [b] Standard deviation is *ca.* 1. η(300 K, kg s^{-1} m^{-1}): CH_2Cl_2: 0.40; $CHCl_3$: 0.55.

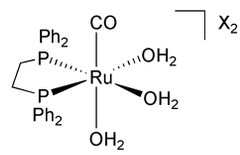

9

Since strong water solvation of the anions does not reduce their actual volume, the relatively large *r*-values for the cations and anions in acetone are likely to result from hydrogen bonding effects. The three complexed water molecules interact with the anions, thereby significantly increasing their relative averaged volumes, while simultaneously increasing the average size of the cations to a lesser extent. Nevertheless, in acetone the cations move at different rates relative to the anions, so that the H-bonding is not 100%.

These examples clearly indicate the ease with which PGSE data can monitor anion interactions with alcohol type ligands.

Ion pairing

In the course of developing our PGSE methodology we noticed a strong solvent dependence[14] of the *D* value for the complexes **10** and **11** [24] in CD_2Cl_2 and $CDCl_3$.

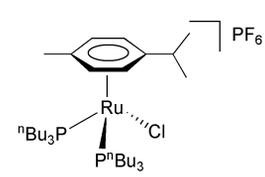

10

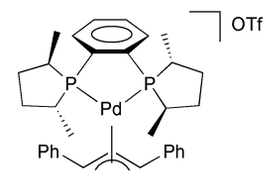

11

The *D*-values for the PF_6^- and $CF_3SO_3^-$ anions (determined *via* ^{19}F measurements) in CD_2Cl_2 suggest that these are moving much faster than their respective cations (see Table 4). In $CDCl_3$, the two species move at almost identical rates. Obviously, the change of solvent from dichloromethane to chloroform has resulted in a tight ion pair such that the two smaller anions now diffuse at about the same rate as their cations. Once again the diffusion constant measured *via* ^{19}F and that obtained from the ^{1}H data are almost identical. In CD_2Cl_2 the diffusion constants for the cation and anion are larger and quite different. We have found this type of effect, *i.e.*, tight ion-pairing in $CDCl_3$ to be general[21,23,25] and show extensive solvent dependent data in Tables 5 and 6, for iridium compounds **13** and **14** (based on **12**, see Scheme 2) and the Ru(II) complex **15**.

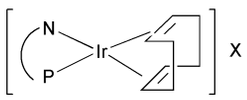

[Ir(1,5-COD)(**12**)]X

13b X = PF_6

13c X = OTf

1 atm. H_2 | methanol

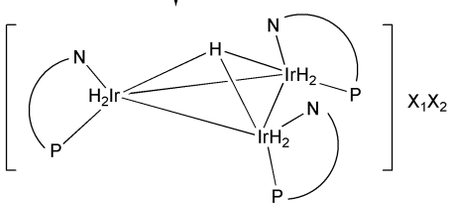

$[Ir_3(\mu^3\text{-H})\ (H)_6(\mathbf{12})_3]X_1X_2$

14a X_1 = PF_6 X_2 = OTf

14b $X_1 = X_2 = PF_6$

14c $X_1 = X_2$ = OTf

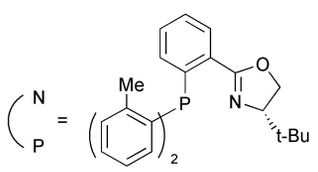

12

Scheme 2 Iridum oxazoline chemistry.

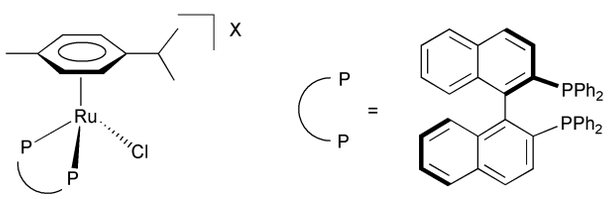

15

One way to demonstrate this dichloromethane–chloroform solvent dependence involves comparing ^1H–^{19}F HOESY spectra for the same species in these solvents. We expect, and find, stronger NOEs (more intense cross-peaks) in chloroform, see Fig. 6.[23,25] The HOESY spectrum of tri-nuclear iridium derivative **14** in methanol solution afforded no observable ^1H–^{19}F NOE cross-peaks, as expected for a strongly solvating solvent. Interestingly, for **14**, in $CDCl_3$, we find no cross-peaks from the three non-equivalent hydride ligands to the $CF_3SO_3^-$ trifluoromethyl group. The most intense contacts arise from the interactions with the aryl groups, so that we assume that the anion approaches the cation *via* the 1,2-disubstituted aryl backbone moiety.

Our *D*-values should not be interpreted to mean that there is *no* ion pairing in dichloromethane. On the contrary, measurements in this solvent routinely reveal hydrodynamic radii (for the small anions) that are much larger than those found in, *e.g.*, methanol. Dichloromethane represents yet another solvent where equilibria exist.

An anion effect on catalysis

Chiral oxazoline complexes of the late transition metals are recognized as successful enantioselective catalysts in an increasing number of organic transformations.[26–28] Specifically, Pfaltz

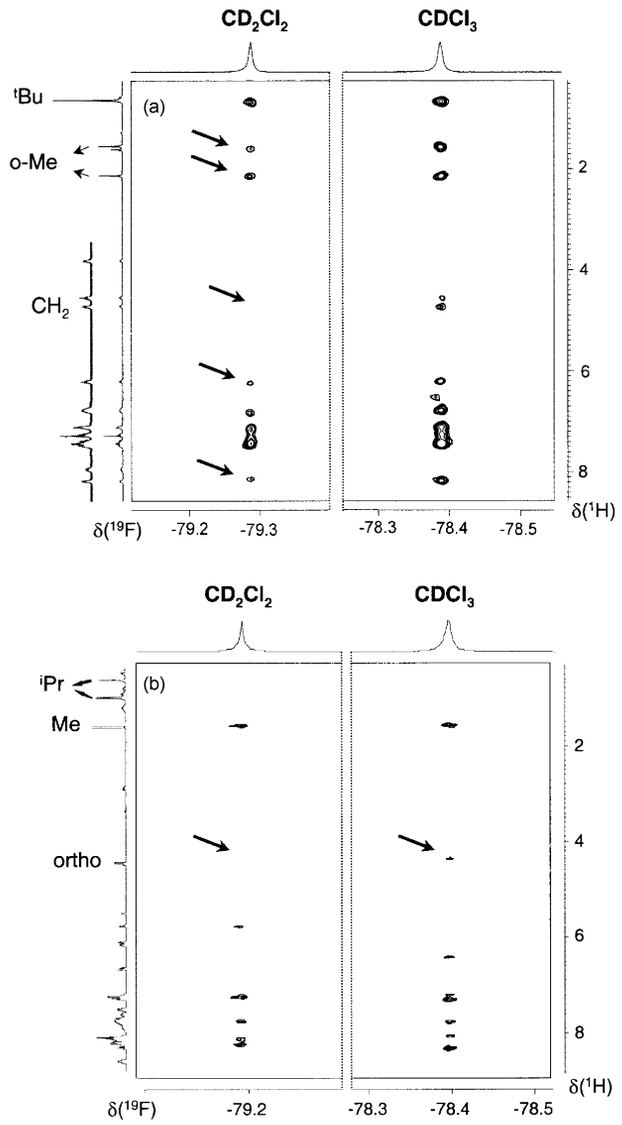

Fig. 6 ^1H–^{19}F HOESY spectra in CD_2Cl_2 and $CDCl_3$, of the tri-nuclear Ir-compound, **14c** (left) and the Ru(II) *p*-cymene Binap complex, **15c** (right), both showing the different Overhauser contacts between cation and $CF_3SO_3^-$ anion. In both comparisons there are more and stronger contacts in $CDCl_3$.

and co-workers have found that the Ir(I) catalyst precursor Ir(1,5-COD)(**12**)](BArF) hydrogenates tri-substituted olefins in dichloromethane with excellent enantioselectivity [see eqn. (3)].[29] However, the lifetime and the activity of this catalyst have been shown to depend on the nature of the anion, with PF_6^- having a rather shorter lifetime than the analogous $BArF^-$ derivative.

It is known that mono-nuclear iridium complexes, *e.g.*, [Ir(1,5-COD)(P,N ligand types)](anion), react under hydrogen in solution to afford tri-nuclear hydrido-cluster complexes,[30,31] which are thought not to be catalytically active in hydrogenation chemistry. We have recently prepared several tri-nuclear clusters, **14**,[32] from the 1,5-COD complexes, as shown in Scheme 2, determined both the solid-and solution state structures (X-ray diffraction and NOESY methods) and shown these *not* to be active catalysts.

The diffusion results for the Ir(I) 1,5-COD model precursor, **13**, paint a picture with respect to the possible difference between PF_6^- and the analogous $BArF^-$ derivative (see Table 5). The $BArF^-$ anion slows the motions of the cation somewhat suggesting some ion-pairing. The PF_6^- anion moves rather easily and does not slow the cation. The volume of the cation in the PF_6^- analog is found to be the same in methanol (strong

Table 5 *D*- and r_H-values for **13a**–**e** and **14a**–**c**[a] in CD_3OD, CD_2Cl_2, $CDCl_3$ and $ClCH_2CH_2Cl$

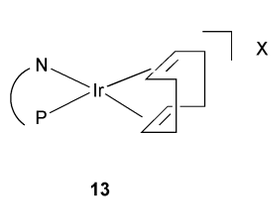

13

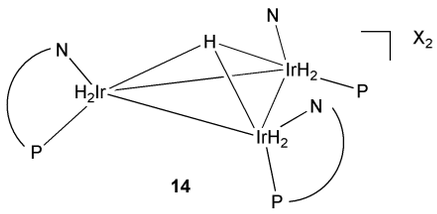

14

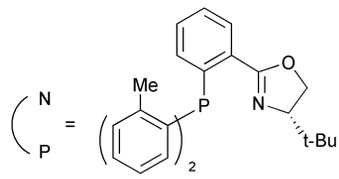

Compound	Fragment	CD_3OD		CD_2Cl_2		$CDCl_3$		$ClCH_2CH_2Cl$	
		D[b]	r_H[c]/Å	D[b]	r_H[c]/Å	D[b]	r_H[c]/Å	D[b]	r_H[c]/Å
13a BF_4	Cation (^{1}H)	7.58	5.5	9.72	5.5	7.23	5.7	5.44	5.4
	Anion (^{19}F)	16.62	2.5	13.79	3.9	7.43	5.6	8.52	3.4
13b PF_6	Cation (^{1}H)	7.57	5.5	9.72	5.5	7.13	5.8	5.37	5.4
	Anion (^{19}F)	15.82	2.6	13.27	4.0	7.21	5.8	8.00	3.6
13c OTf	Cation (^{1}H)	7.65	5.5	9.71	5.5	7.04	5.9	5.36	5.4
	Anion (^{19}F)	12.95	3.2	12.52	4.3	7.05	5.9	7.67	3.8
13d $B(C_6F_5)_4$	Cation (^{1}H)	7.62	5.5	9.24	5.8	6.06	6.9	5.17	5.7
	Anion (^{19}F)	7.69	5.4	9.12	5.9	5.91	7.0	5.08	5.8
	Cation (^{1}H)	7.55	5.5	9.20	5.8	5.70	7.3	5.09	5.7
13e BArF	Anion (^{1}H)	6.77	6.2	8.40	6.4	5.63	7.4		
	Anion (^{19}F)	6.67	6.2	8.43	6.4	5.59	7.4	4.71	6.2
14a $(PF_6)(OTf)$	Cation (^{1}H)	5.09	8.2	6.34	8.3	4.64	8.9	3.50	8.3
	PF_6 (^{19}F)	15.16	2.7	9.65	5.5	4.70	8.8	6.04	4.8
	OTf (^{19}F)	12.34	3.4	9.82	5.5	4.71	8.8	6.19	4.7
14b $(PF_6)_2$	Cation (^{1}H)	5.06	8.2	6.53	8.2	4.94	8.4	3.57	8.2
	Anion (^{19}F)	15.51	2.7	9.57	5.6	5.12	8.1	6.21	4.7
14c $(OTf)_2$	Cation (^{1}H)	5.10	8.2	6.47	8.3	4.33	9.6	3.52	8.3
	Anion (^{19}F)	12.12	3.4	9.84	5.4	4.43	9.4	5.83	5.0

[a] 2 mM. [b] $\times 10^{10}$ m^2 s^{-1}. Estimated using the diffusion coefficient of HDO in D_2O as ref. 33. Standard deviation is *ca.* 6. [c] Standard deviation is *ca.* 1. η(300 K, kg s^{-1} m^{-1}): CH_3OH: 0.526; CH_2Cl_2: 0.410; $CHCl_3$: 0.529; $ClCH_2CH_2Cl$: = 0.751.

Table 6 *D*- and r_H-values for **15a**–**f**[a] in CD_3OD, CD_2Cl_2, $CDCl_3$ and $(CD_3)_2CO$

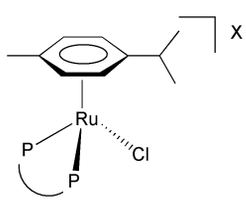

15

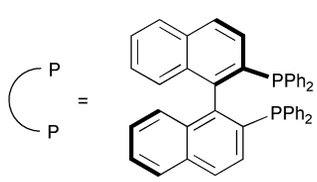

Compound	Fragment	CD_3OD		CD_2Cl_2		$CDCl_3$		$(CD_3)_2CO$	
		D[b]	r_H[c]/Å	D[b]	r_H[c]/Å	D[b]	r_H[c]/Å	D[b]	r_H[c]/Å
15a BF_4	Cation (^{1}H)	5.98	7.0	7.89	6.8	5.89	7.0	10.07	7.2
	Anion (^{19}F)	15.73	2.6	10.95	4.9	5.99	6.9	26.85	2.7
15b OTf	Cation (^{1}H)	5.96	7.0	7.73	6.9	5.93	7.0	9.95	7.3
	Anion (^{19}F)	12.28	3.4	10.46	5.1	6.05	6.9	23.39	3.1
15c BArF	Cation (^{1}H)	5.98	7.0	7.71	6.9	4.78	8.6	9.91	7.3
	Anion (^{19}F)	6.42	6.5	8.05	6.6	4.88	8.5	10.83	6.7
NaBArF	Anion (^{19}F)	6.53	6.3						
15d PF_6	Cation (^{1}H)			7.87	6.8				
	Anion (^{19}F)			10.99	4.9				

[a] 2 mM. [b] $\times 10^{10}$ m^2 s^{-1}. Estimated using the diffusion coefficient of HDO in D_2O as ref. 33. Standard deviation is *ca.* 6. [c] Standard deviation is *ca.* 1. η(300 K, kg s^{-1} m^{-1}): CH_3OH: 0.526; CH_2Cl_2: 0.410; $CHCl_3$: 0.529; $(CH_3)_2CO$: = 0.303.

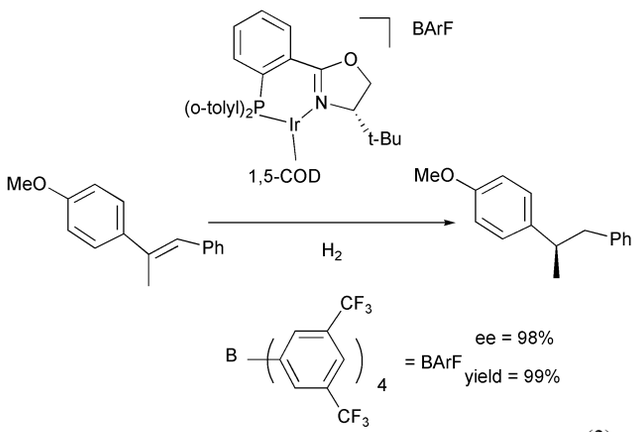

(3)

solvation) as it is in dichloromethane, suggesting a modest interaction with this anion in the latter solvent. If the mechanism of the formation of an inactive Ir_3 cluster requires that two fairly large species associate, and subsequently add yet another large moiety, then, in dichloromethane, these processes are likely to be faster for a complex containing a relatively small rapidly moving anion, such as PF_6^-, than for a larger, partially ion-paired complex with $BArF^-$. This is a sort of steric inhibition to deactivation.

Comments

The ability to rapidly estimate the molecular volume of a metal complex (or a mixture of complexes) represents yet another useful NMR tool. Further, we can use these PGSE methods, together with ^1H–^{19}F HOESY data, to qualitatively investigate problems involving ion-pairing and hydrogen bonding. Admittedly, the problems posed by residence times will often be complicated due to exchange; nevertheless, we believe that PGSE methods offer yet another, complementary tool in an area of chemistry which remains relatively unexplored.

Acknowledgements

P. S. P. thanks the Swiss National Science Foundation, the BBW and the ETH Zurich for financial support and Johnson Matthey for the loan of precious metals. E. M.-V. thanks the Seneca Foundation (Comunidad Autónomona de la Región de Murcia, Spain) for a grant. Special thanks are due to the many colleagues who have generously provided us with compounds and their names appear in the appropriate citations. We would also like to thank Dr. Heinz Rüegger (ETHZ, Zürich) for very helpful discussions and advice.

References

1 C. S. Johnson, Jr., *Prog. Nucl. Magn. Reson. Spectrosc.*, 1999, **34**, 203–256.
2 P. Stilbs, *Prog. Nucl. Magn. Reson. Spectrosc.*, 1987, **19**, 1–45.
3 E. O. Stejskal and J. E. Tanner, *J. Chem. Phys.*, 1965, **42**, 288–292.
4 A. Macchioni, *Eur. J. Inorg. Chem*, 2003, 195–205; A. Macchioni, A. Magistrato, I. Orabona, F. Ruffo, U. Rothlisberger and C. Zuccaccia, *New J. Chem.*, 2003, **27**, 455–458; R. Romeo, L. Fenech, L. M. Scolaro, A. Albinati, A. Macchioni and C. Zuccaccia, *Inorg. Chem.*, 2001, **40**, 3293–3302; C. Zuccaccia, G. Bellachioma, G. Cardaci and A. Macchioni, *Organometallics*, 2000, **19**, 4663–4665; A. Macchioni, G. Bellachioma, G. Cardaci, V. Gramlich, H. Ruegger, S. Terenzi and L. M. Venanzi, *Organometallics*, 1997, **16**, 2139–2145.
5 S. Beck, A. Geyer and H. H. Brintzinger, *Chem. Commun.*, 1999, 2477–2478.
6 B. Olenyuk, M. D. Levin, J. A. Whiteford, J. E. Shield and P. J. Stang, *J. Am. Chem. Soc.*, 1999, **121**, 10434–10435; C. B. Gorman, J. C. J. Smith, M. W. Hager, B. L. Parkhurst, H. Sierzputowska-Gracz and C. A. Haney, *J. Am. Chem. Soc.*, 1999, **121**, 9958–9966.
7 O. Mayzel and Y. Cohen, *J. Chem. Soc., Chem. Commun.*, 1994, 1901–1902.
8 R. E. Hoffman, E. Shabtai, M. Rabinovitz, V. S. Iyer, K. Müllen, A. K. Rai, E. Bayrd and L. T. Scott, *J. Chem. Soc., Perkin Trans. 2*, 1998, 1659–1664.
9 Q. Jiang, H. Rüegger and L. M. Venanzi, *Inorg. Chim. Acta*, 1999, **290**, 64–79.
10 R. M. Stoop, S. Bachmann, M. Valentini and A. Mezzetti, *Organometallics*, 2000, **19**, 4117–4126.
11 N. E. Schlörer, E. J. Cabrita and S. Berger, *Angew. Chem., Int. Ed.*, 2002, **41**, 107–109; E. J. Cabrita and S. Berger, *Magn. Reson. Chem.*, 2001, **39**, S142–S148; I. Keresztes and P. G. Williard, *J. Am. Chem. Soc.*, 2000, **122**, 10228–10229.
12 D. Drago, P. S. Pregosin and A. Pfaltz, *Chem. Commun.*, 2002, 286–287; M. Valentini, P. S. Pregosin and H. Rüegger, *J. Chem. Soc., Dalton Trans.*, 2000, 4507–4510; M. Valentini, P. S. Pregosin and H. Rüegger, *Organometallics*, 2000, **19**, 2551–2555; A. Pichota, P. S. Pregosin, M. Valentini, M. Wörle and D. Seebach, *Angew. Chem., Int. Ed. Engl.*, 2000, **39**, 153–156.
13 Y. Chen, M. Valentini, P. S. Pregosin and A. Albinati, *Inorg. Chim. Acta*, 2002, **327**, 4–14.
14 M. Valentini, H. Rüegger and P. S. Pregosin, *Helv. Chim. Acta*, 2001, **84**, 2833–2853.
15 J. E. Tanner, *J. Chem. Phys.*, 1970, **52**, 2523.
16 T. J. Geldbach, P. S. Pregosin, A. Albinati and F. Rominger, *Organometallics*, 2001, **20**, 1932.
17 C. J. den Reijer, M. Wörle and P. S. Pregosin, *Organometallics*, 2000, **19**, 309.
18 J. S. Song, D. J. Szalda and R. M. Bullock, *Organometallics*, 2001, **20**, 3337.
19 Jerschow and N. Müller, *J. Magn. Reson.*, 1997, **125**, 372; N. Esturau, F. Sánchez-Ferrando, J. A. Gavin, C. Roumestand, M.-A. Delsuc and T. Parella, *J. Magn. Reson.*, 2001, **153**, 48; N. Hedin and I. Furó, *J. Magn. Reson.*, 1998, **131**, 126; E. Martinez-Viviente and P. S. Pregosin, *Helv. Chim. Acta*, accepted.
20 G. R. Eastham, B. T. Heaton, J. A. Iggo, R. P. Tooze, R. Whymann and S. Zacchini, *Chem. Commun.*, 2000, 609; W. Clegg, G. R. Eastam, M. R. J. Elsegood, B. T. Heaton, J. A. Iggo, R. P. Tooze, R. Whymann and S. Zacchini, *J. Chem. Soc., Dalton Trans.*, 2002, **17**, 3300.
21 E. Martinez-Viviente, H. Rügger, P. S. Pregosin and J. Lopez-Serrano, *Organometallics*, 2002, **21**, 5841.
22 M. F. Mahon, M. K. Whittlesey and P. T. Wood, *Organometallics*, 1999, **18**, 4068; M. D. Hargreaves, M. F. Mahon and M. K. Whittlesey, *Inorg. Chem.*, 2002, **41**, 3137.
23 P. G. Anil Kumar, P. S. Pregosin, J. M. Goicoechea and M. K. Whittlesey, *Organometallics*, accepted.
24 D. Drago and P. S. Pregosin, *J. Chem. Soc., Dalton Trans.*, 2000, 3191.
25 E. Martinez-Viviente and P. S. Pregosin, *Inorg. Chem.*, 2003, **42**, 2209.
26 G. Helmchen and A. Pfaltz, *Acc. Chem. Res.*, 2000, **33**, 336–345; H. Tye, *J. Chem. Soc., Perkin Trans.1*, 2000, 275–298; A. K. Ghosh, P. Mathivanan and J. Cappiello, *Tetrahedron: Asymmetry*, 1998, **9**, 1–45; all offer useful overviews.
27 G. Helmchen, *J. Organomet. Chem.*, 1999, **576**, 203–214; T. Langer and G. Helmchen, *Tetrahedron Lett.*, 1996, **37**, 1381–1384.
28 A. Lightfoot, P. Schnider and A. Pfaltz, *Angew. Chem., Int. Ed. Engl.*, 1998, **37**, 2897–2899; D. G. Blackmond, A. Lightfoot, A. Pfaltz, T. Rosner, P. Schnider and N. Zimmermann, *Chirality*, 2000, **12**, 442–449; P. G. Cozzi, N. Zimmermann, R. Hilgraf, S. Schaffner and A. Pfaltz, *Adv. Synth. Catal.*, 2001, **343**, 450–454; J. Blankenstein and A. Pfaltz, *Angew. Chem., Int. Ed.*, 2001, **40**, 4445–4447; F. Menges and A. Pfaltz, *Adv. Synth. Catal.*, 2002, **344**, 40–44.
29 A. Pfaltz, J. Blankenstein, R. Hilgraf, E. Hörmann, S. McIntyre, F. Menges, M. Schönleber, S. P. Smidt, B. Wüstenberg and N. Zimmermann, *Adv. Synth. Catal.*, 2003, **345**, 33–43.
30 D. F. Chodosh, R. H. Crabtree, H. Felkin and G. E. Morris, *J. Organomet. Chem.*, 1978, **161**, C67–C70.
31 H. Wang, A. L. Casalnuovo, B. J. Johnson, A. M. Mueting and L. H. Pignolet, *Inorg. Chem.*, 1988, **27**, 325–331; H. H. Wang and L. H. Pignolet, *Inorg. Chem.*, 1980, **19**, 1470.
32 P. S. Smidt, A. Pfaltz, E. Martínez-Viviente, P. S. Pregosin and A. Albinati, *Organometallics*, 2003, **22**, 1000–1009.
33 H. J. W. Tyrrell and K. R. Harris, *Diffusion in Liquids*, Butterworths, London, 1984.